2017

A Numerical Study of Construction of Honey Bee Comb

Pamela Guerrero

Pamela C. Guerrero
Murray State University

A Numerical Study of Construction of Honey Bee Comb

A Thesis

Presented to

the Faculty of the Department of Mathematics and Statistics

Murray State University

Murray, Kentucky

In Partial Fulfillment

of the Requirements for the Degree

of Master of Science

by

Pamela Guerrero

April 24, 2017

Title

DATE APPROVED: ______________________

____
Dr. Donald Adongo, Thesis Advisor

____
Dr. Maeve Lewis McCarthy, Thesis Committee

____
Dr. Manoj Pathak, Thesis Committee

____
Dr. Kevin Revell, Graduate Coordinator, Jones College of Sci., Eng., and Tech.

____
Dr. Stephen Cobb, Dean, Jones College of Sci., Eng., and Tech.

____
Dr. Robert Pervine, University Graduate Coordinator

____
Dr. Renae Duncan, Provost

– ACKNOWLEDGMENT PAGE

First of all, I would like to thank Dr. Donald Adongo for his guidance, dedication, and patience in seeing this thesis to its completion. You have taught me a great deal and helped me see a subset of mathematics in a more connected and in depth way. I am grateful to Dr. Maeve McCarthy for the opportunities she has given me, two of which are her offering of an independent study in mathematical biology and her opening the door for the thesis route. I want to thank Jordan Culp for the inspiration to begin this project and giving me a good jump start. Lastly, but certainly not least, I want to thank my husband Brian Boyd for being a source of support in this path I chose, my Mother for her understanding, and my children, Bryson and Corrina for keeping me focused on what is important in life.

Abstract

We use finite difference methods in the treatment of an existing system of partial differential equations that captures the dynamics of parallel honeycomb construction in a bee hive. We conduct an uncertainty analysis by calculating the partial rank correlation coefficient for the parameters to find which are most important to the outcomes of the model. We then use an eFAST method to determine both the individual and total sensitivity index for the parameters. Afterwards we examine our numerical model under varying initial conditions and parameter values, and compare ratios found from local data with the golden mean by fitting images of the combs with ellipses and then calculating the length of the major and minor axes.

Contents

Chapter 1

Introduction

It is no secret that pollinators, such as honey bees, play a vital role in the production of food for the human species. In 2005 the economic value of pollinators worldwide was estimated at \$162 billion, 9.5% of the value of the world agriculture production used for human food. Without pollinators the production of fruits, vegetables, and stimulants would have been clearly below the year's consumption levels [12]. In this thesis, we research the mathematics behind honeycomb construction.

The building behavior of social insects, such as ants, bees, wasps, and termites, is a complex and social phenomenon which results in the construction of nests whose size and complexity would be impossible for just a few insects to build alone. In particular, *Apis mellifera*, the European honey bee has a strong tendency to construct parallel combs in a hive. It begins by worker bees randomly depositing small balls of wax on the ceiling; the presence of both the bees and the wax attract more bees to join in the effort. Some deposits grow more quickly than others and some are deserted altogether. Whenever an arbitrary ball of new wax is deposited this can be understood as a small fluctuation and the deposit may be enhanced and begin to form an oval shape that increases in length and determines the orientation of the construction or it may be abandoned. Future combs will be formed on either side and a parallelism within the combs will become evident. The bees are attracted to the wax, an autocatalytic reaction, but at the same time they are attracted to the other bees who are waving their legs as a signal for workers to join them in forming waxer bee chains. The role of these chains is to regulate construction and to maintain the parallelism of the combs. They allow construction to be coordinated at a distance much further along than the length of a single bee; however, the orientation of the chains themselves are dictated by the orientation of the initial stages of construction [2]. This parallel comb construction has been modeled mathematically and considered using computer simulations. The purpose of this thesis is to study this same model by a different method, finite differences, in hopes of creating an updated and more accurate graphical interpretation.

We begin by introducing the partial differential equation system which includes equations for the change in the density with respect to time based on their spatial orientation and an equation for the change in wax concentration with respect to time. A detailed explanation of the parameters used is given. In the following chapter the details of how we arrive at our finite difference scheme are provided and we calculate the truncation error introduced by our method. To increase our understanding of the model we study the steady states and in particular notice the effect of the parameter values on these steady states. MatLab software is used to conduct uncertainty and sensitivity analysis for the purpose of examining the range of the parameters. For a subset of the parameters, we use a Latin hypercube sampling technique then calculate the partial rank correlation coefficient for the sampled parameters and determine for each parameter how a change in its value affects the outputs of the model. We can get a general idea of the effect that each parameter has on the model by examining the graphs of outputs versus sampled parameter values. We follow with an extended Fourier amplitude test (eFAST) to further study the effects of the parameters. With the eFAST method we can look at both the individual and total effects for each parameter. We conclude by examining the measurements of honeycombs collected in west Tennessee and comparing the ratio of the major and minor axes of overlaid ellipses with the golden mean. We also extend the study of the model by considering the graphs of the outputs and searching for the parameter values and initial conditions that best reproduced the parallelism within the hive and the elliptical nature of the combs.

1.1 PDE Model

$$\partial_t H - \theta \nabla^2 H = \phi - \tau H + m_x H \tag{1.1.1}$$

$$\partial_t V - \theta \nabla^2 V = \phi - \tau V + m_y V \tag{1.1.2}$$

$$\partial_t C - (H+V) D \nabla^2 C = \alpha(H+V) - \nu C \tag{1.1.3}$$

$$m_x = \beta(HV - V^2) + \delta C + \gamma \partial_x^2 C + \varepsilon \partial_x^4 C \tag{1.1.4}$$

$$m_y = \beta(HV - H^2) + \delta C + \gamma \partial_y^2 C + \varepsilon \partial_y^4 C \tag{1.1.5}$$

Here ∇^2 represents the two dimensional Laplacian, and the independent and dependent variables are given by the following:

- C represents the quantity of deposited wax
- H represents the average density of bees parallel to XZ plane
- V represents the average density of bees parallel to YZ plane
- x and y are the spatial variables
- t represents the time that has passed since the honeycomb construction began

The parameters and terms in the model are explained below:

- θ represents the coefficient of difussion control

- ϕ represents the flux of differently oriented bees which come into the considered volume on the top of the beehive
- $\tau H,\ \tau V$ correspond to the loss of some bees which leave or change orientation
- $\alpha(H+V)$ gives the change in the wax distribution caused by the newly brought wax
- νC represents the removed or fallen wax
- $(H+V)D\nabla^2 C$ represents the wax deposited due to imitation
- $\beta(HV-(H/V)^2)$ accounts for the local coupling between H and V which contains respectively the gain term corresponding to the reorientation of the V/H bees due to the presence of the H/V bees and the loss term which corresponds to the reorientation of the H/V bees through an "autocatalitic reaction"
- $\delta C+\gamma\partial^2_{x/y}C+\varepsilon\partial^4_{x/y}C$ describes the attraction of the bees to the wax and various gradients of the wax distribution

Equivalently the model can be written in the form given below:

$$\partial_t H = \theta(\partial_{xx}H+\partial_{yy}H)+\phi-\tau H+m_x H \quad (1.1.6)$$

$$\partial_t V = \theta(\partial_{xx}V+\partial_{yy}V)+\phi-\tau V+m_y V \quad (1.1.7)$$

$$\partial_t C = (H+V)D(\partial_{xx}C+\partial_{yy}C)+\alpha(H+V)-\nu C \quad (1.1.8)$$

$$m_x = \beta(HV-H^2)+\delta C+\gamma\partial_x^2 C+\varepsilon\partial_x^4 C \quad (1.1.9)$$

$$m_y = \beta(HV-V^2)+\delta C+\gamma\partial_y^2 C+\varepsilon\partial_y^4 C \quad (1.1.10)$$

1.2 Stationary Solutions

To find the stationary solutions of the system the time and space derivatives are set to zero.

$$0 = \phi - \tau H + m_x H \tag{1.2.1}$$

$$0 = \phi - \tau V + m_y V \tag{1.2.2}$$

$$0 = \alpha(H+V) - \nu C \tag{1.2.3}$$

$$m_x = \beta(HV - V^2) + \delta C \tag{1.2.4}$$

$$m_y = \beta(HV - H^2) + \delta C \tag{1.2.5}$$

There are three possibilities for the steady states of the density of bees and in all cases the concentration of wax stays the same.

$$H = \frac{\phi}{\tau} \quad V = \frac{\phi}{\tau} \tag{1.2.6}$$

$$H = \frac{\phi}{\tau} + (\frac{\phi^2}{\tau^2} - \frac{\tau}{2\beta})^{1/2} \quad V = \frac{\phi}{\tau} - (\frac{\phi^2}{\tau^2} - \frac{\tau}{2\beta})^{1/2} \tag{1.2.7}$$

$$H = \frac{\phi}{\tau} - (\frac{\phi^2}{\tau^2} - \frac{\tau}{2\beta})^{1/2} \quad V = \frac{\phi}{\tau} + (\frac{\phi^2}{\tau^2} - \frac{\tau}{2\beta})^{1/2} \tag{1.2.8}$$

$$C = \frac{\alpha}{\nu}(H+V) = \frac{2\alpha\phi}{\nu\tau} \tag{1.2.9}$$

Solutions (1.2.6) represents the steady state when the density of bees parallel to the XZ plane (H) and YZ plane (V) are the same. In solution (1.2.7) H has the larger value and in solution (1.2.8) V has the larger value. To stay in the feasible region where H, V, and C will be greater than or equal to zero we must have $\phi > \phi_c$ where $\phi_c = \left(\frac{\tau^2}{2\beta}\right)^{1/2}$. If $\phi_c < \phi$ the only stationary solution that exists is (1.2.6).

Chapter 2

Numerical Scheme

A PDE model for honeycomb construction that captures several of the nuances of bee building behavior has been proposed and previously implemented with a spectral algorithm based on a modified thin-sheet gain scheme and a fast Fourier transform technique for treatment of the equations [15]. With today's easy access to advanced computers finite differences are fairly easy to implement for a numerical solution to PDE's. In this thesis we hope to gain equivalent or better results using this technique.

We begin this chapter by applying the finite difference technique to discretize the model. We use a forward difference approximation for the time derivatives and central difference approximations for the second and fourth spatial derivatives, and we solve the resulting equations for the latest time step. Because finite differences uses approximations for the derivatives we follow up by calculating the error that was introduced with the method by using Taylor series expansions and then determining the order for the truncation error.

2.1 Finite Difference Scheme

The partial derivatives are approximated by

$$
\begin{aligned}
\partial_t H &\approx \frac{H(x_k, y_i, t_{n+1}) - H(x_k, y_i, t_n)}{\Delta t} \\
\partial_t V &\approx \frac{V(x_k, y_i, t_{n+1}) - V(x_k, y_i, t_n)}{\Delta t} \\
\partial_t C &\approx \frac{C(x_k, y_i, t_{n+1}) - C(x_k, y_i, t_n)}{\Delta t} \\
\nabla^2 H &\approx \frac{H(x_{k+1}, y_i, t_n) - 2H(x_k, y_i, t_n) + H(x_{k-1}, y_i, t_n)}{(\Delta x)^2} \\
&\quad + \frac{H(x_k, y_{i+1}, t_n) - 2H(x_k, y_i, t_n) + H(x_k, y_{i-1}, t_n)}{(\Delta y)^2} \\
\nabla^2 V &\approx \frac{V(x_{k+1}, y_i, t_n) - 2V(x_k, y_i, t_n) + V(x_{k-1}, y_i, t_n)}{(\Delta x)^2} \\
&\quad + \frac{V(x_k, y_{i+1}, t_n) - 2V(x_k, y_i, t_n) + V(x_k, y_{i-1}, t_n)}{(\Delta y)^2} \\
\nabla^2 C &\approx \frac{C(x_{k+1}, y_i, t_n) - 2C(x_k, y_i, t_n) + C(x_{k-1}, y_i, t_n)}{(\Delta x)^2} \\
&\quad + \frac{C(x_k, y_{i+1}, t_n) - 2C(x_k, y_i, t_n) + C(x_k, y_{i-1}, t_n)}{(\Delta y)^2} \\
\partial_x^2 C &\approx \frac{C(x_{k+1}, y_i, t_n) - 2C(x_k, y_i, t_n) + C(x_{k-1}, y_i, t_n)}{(\Delta x)^2} \\
\partial_y^2 C &\approx \frac{C(x_k, y_{i+1}, t_n) - 2C(x_k, y_i, t_n) + C(x_k, y_{i-1}, t_n)}{(\Delta y)^2}
\end{aligned}
\tag{2.1.1}
$$

$$\partial_x^4 C \approx \frac{C(x_{k+2}, y_i, t_n) - 4C(x_{k+1}, y_i, t_n) + 6C(x_k, y_i, t_n) - 4C(x_{k-1}, y_i, t_n) + C(x_{k-2}, y_i, t_n)}{(\Delta x)^4}$$

$$\partial_y^4 C \approx \frac{C(x_k, y_{i+2}, t_n) - 4C(x_k, y_{i+1}, t_n) + 6C(x_k, y_i, t_n) - 4C(x_k, y_{i-1}, t_n) + C(x_k, y_{i-2}, t_n)}{(\Delta y)^4}$$

For convenience, we let $U_{k,i}^n = U(x_k, y_i, t_n)$ and then substitute the partial derivative approximations into the model.

So equations (1.1.6 – 1.1.10) become

$$\begin{aligned} \frac{H_{k,i}^{n+1} - H_{k,i}^n}{\Delta t} &= \theta\Big[\frac{H_{k+1,i}^n - 2H_{k,i}^n + H_{k-1,i}^n}{(\Delta x)^2} + \frac{H_{k,i+1}^n - 2H_{k,i}^n + H_{k,i-1}^n}{(\Delta y)^2}\Big] \\ &+ \phi - \tau H_{k,i}^n + \hat{m}_x H_{k,i}^n \end{aligned} \tag{2.1.2}$$

$$\begin{aligned} \frac{V_{k,i}^{n+1} - V_{k,i}^n}{\Delta t} &= \theta\Big[\frac{V_{k+1,i}^n - 2V_{k,i}^n + V_{k-1,i}^n}{(\Delta x)^2} + \frac{V_{k,i+1}^n - 2V_{k,i}^n + V_{k,i-1}^n}{(\Delta y)^2}\Big] \\ &+ \phi - \tau V_{k,i}^n + \hat{m}_y V_{k,i}^n \end{aligned} \tag{2.1.3}$$

$$\begin{aligned} \frac{C_{k,i}^{n+1} - C_{k,i}^n}{\Delta t} &= (H_{k,i}^n + V_{k,i}^n) D \Big[\frac{C_{k+1,i}^n - 2C_{k,i}^n + C_{k-1,i}^n}{(\Delta x)^2} \\ &+ \frac{C_{k,i+1}^n - 2C_{k,i}^n + C_{k,i-1}^n}{(\Delta y)^2}\Big] + \alpha(H_{k,i}^n + V_{k,i}^n) - \nu C_{k,i}^n \end{aligned} \tag{2.1.4}$$

$$\begin{aligned} \hat{m}_x &= \beta(H_{k,i}^n V_{k,i}^n - (V_{k,i}^n)^2) + \delta C_{k,i}^n + \gamma \frac{C_{k+1,i}^n - 2C_{k,i}^n + C_{k-1,i}^n}{(\Delta x)^2} \\ &+ \varepsilon \frac{C_{k+2,i}^n - 4C_{k+1,i}^n + 6C_{k,i}^n - 4C_{k-1,i}^n + C_{k-2,i}^n}{(\Delta x)^4} \end{aligned} \tag{2.1.5}$$

$$\begin{aligned} \hat{m}_y &= \beta(H_{k,i}^n V_{k,i}^n - (H_{k,i}^n)^2) + \delta C_{k,i}^n + \gamma \frac{C_{k,i+1}^n - 2C_{k,i}^n + C_{k,i-1}^n}{(\Delta y)^2} \\ &+ \varepsilon \frac{C_{k,i+2}^n - 4C_{k,i+1}^n + 6C_{k,i}^n - 4C_{k,i-1}^n + C_{k,i-2}^n}{(\Delta y)^4} \end{aligned} \tag{2.1.6}$$

Then solving the model for time $= t_{n+1}$ yields the following equations:

$$\begin{aligned} H^{n+1}_{k,i} &= \Delta t\Big(\theta\Big[\frac{H^n_{k+1,i} - 2H^n_{k,i} + H^n_{k-1,i}}{(\Delta x)^2} + \frac{H^n_{k,i+1} - 2H^n_{k,i} + H^n_{k,i-1}}{(\Delta y)^2}\Big] \\ &\quad + \phi - \tau H^n_{k,i} + \hat{m}_x H^n_{k,i}\Big) + H^n_{k,i} \end{aligned} \tag{2.1.7}$$

$$\begin{aligned} V^{n+1}_{k,i} &= \Delta t\Big(\theta\Big[\frac{V^n_{k+1,i} - 2V^n_{k,i} + V^n_{k-1,i}}{(\Delta x)^2} + \frac{V^n_{k,i+1} - 2V^n_{k,i} + V^n_{k,i-1}}{(\Delta y)^2}\Big] \\ &\quad + \phi - \tau V^n_{k,i} + \hat{m}_y V^n_{k,i}\Big) + V^n_{k,i} \end{aligned} \tag{2.1.8}$$

$$\begin{aligned} C^{n+1}_{k,i} &= \Delta t\Big((H^n_{k,i} + V^n_{k,i})D\Big[\frac{C^n_{k+1,i} - 2C^n_{k,i} + C^n_{k-1,i}}{(\Delta x)^2} \\ &\quad + \frac{C^n_{k,i+1} - 2C^n_{k,i} + C^n_{k,i-1}}{(\Delta y)^2}\Big] \\ &\quad + \alpha(H^n_{k,i} + V^n_{k,i}) - \nu C^n_{k,i}\Big) + C^n_{k,i} \end{aligned} \tag{2.1.9}$$

$$\begin{aligned} \hat{m}_x &= \beta(H^n_{k,i}V^n_{k,i} - (V^n_{k,i})^2) + \delta C^n_{k,i} + \gamma\ \frac{C^n_{k+1,i} - 2C^n_{k,i} + C^n_{k-1,i}}{(\Delta x)^2} \\ &\quad + \varepsilon\frac{C^n_{k+2,i} - 4C^n_{k+1,i} + 6C^n_{k,i} - 4C^n_{k-1,i} + C^n_{k-2,i}}{(\Delta x)^4} \end{aligned} \tag{2.1.10}$$

$$\begin{aligned} \hat{m}_y &= \beta(H^n_{k,i}V^n_{k,i} - (H^n_{k,i})^2) + \delta C^n_{k,i} + \gamma\ \frac{C^n_{k,i+1} - 2C^n_{k,i} + C^n_{k,i-1}}{(\Delta y)^2} \\ &\quad + \varepsilon\frac{C^n_{k,i+2} - 4C^n_{k,i+1} + 6C^n_{k,i} - 4C^n_{k,i-1} + C^n_{k,i-2}}{(\Delta y)^4} \end{aligned} \tag{2.1.11}$$

which defines our finite difference scheme.

2.2 Truncation Error

To determine the local truncation errors, τ_n, we look at the error when the exact solution is applied to the difference scheme. We define the truncation error for H(x,y,t), V(x,y,t) and C(x,y,t) by the following:

$$\begin{aligned}\tau_n^H &= \frac{H(x,y,t+\Delta t)-H(x,y,t)}{\Delta t}-\theta\Big[\frac{H(x+\Delta x,y,t)-2H(x,y,t)+H(x-\Delta x,y,t)}{(\Delta x)^2}\\ &\quad+\frac{H(x,y+\Delta y,t)-2H(x,y,t)+H(x,y-\Delta y,t)}{(\Delta y)^2}\Big]\\ &\quad-\phi+\tau H(x,y,t)-m_xH(x,y,t)\end{aligned} \tag{2.2.1}$$

$$\begin{aligned}\tau_n^V &= \frac{V(x,y,t+\Delta t)-V(x,y,t)}{\Delta t}-\theta\Big[\frac{V(x+\Delta x,y,t)-2V(x,y,t)+V(x-\Delta x,y,t)}{(\Delta x)^2}\\ &\quad+\frac{V(x,y+\Delta y,t)-2V(x,y,t)+V(x,y-\Delta y,t)}{(\Delta y)^2}\Big]\\ &\quad-\phi+\tau V(x,y,t)-m_yV(x,y,t)\end{aligned} \tag{2.2.2}$$

$$\begin{aligned}\tau_n^C &= \frac{C(x,y,t+\Delta t)-C(x,y,t)}{\Delta t}-(H(x,y,t)+V(x,y,t))\\ &\quad D\Big[\frac{C(x+\Delta x,y,t)-2C(x,y,t)+C(x-\Delta x,y,t)}{(\Delta x)^2}\\ &\quad+\frac{C(x,y+\Delta y,t)-2C(x,y,t)+C(x,y-\Delta y,t)}{(\Delta y)^2}\Big]\\ &\quad-\alpha(H(x,y,t)+V(x,y,t))+\nu C(x,y,t)\end{aligned} \tag{2.2.3}$$

We use Taylor series expansion to obtain expressions for the truncation errors. Now,

$$\begin{aligned}\frac{C(x,y,t+\Delta t)-C(x,y,t)}{\Delta t} &= \frac{1}{\Delta t}\Big[\Delta t C_t + \frac{(\Delta t)^2}{2!}C_{tt} + \frac{(\Delta t)^3}{3!}C_{ttt} + \dots\Big] \\ &= C_t + \frac{\Delta t}{2!}C_{tt} + \frac{(\Delta t)^2}{3!}C_{ttt} + \dots\end{aligned}$$

Let,

$$E_c = \frac{C(x+\Delta x,y,t)-2C(x,y,t)+C(x-\Delta x,y,t)}{(\Delta x)^2} \tag{2.2.4}$$

Then

$$\begin{aligned}E_c &= \frac{1}{(\Delta x)^2}\Big[C + \Delta x C_x + \frac{(\Delta x)^2}{2!}C_{xx} + \frac{(\Delta x)^3}{3!}C_{xxx} + \dots - 2C + C - \Delta x C_x \\ &\quad + \frac{(\Delta x)^2}{2!}C_{xx} - \frac{(\Delta x)^3}{3!}C_{xxx} + \dots\Big] \\ &= \frac{1}{(\Delta x)^2}\Big[\frac{2(\Delta x)^2}{2!}C_{xx} + \frac{2(\Delta x)^4}{4!}C_{xxxx} + \dots\Big] \\ &= C_{xx} + \frac{2(\Delta x)^2}{4!}C_{xxxx} + \dots \end{aligned} \tag{2.2.5}$$

Similarly,

$$\frac{C(x,y+\Delta y,t)-2C(x,y,t)+C(x,y-\Delta y,t)}{(\Delta y)^2} = C_{yy} + \frac{2(\Delta y)^2}{4!}C_{yyyy} + \dots \tag{2.2.6}$$

There are equivalent equations for V and H.

Substituting the Taylor Series Expansions into (2.2.1 – 2.2.3) we have the following:

$$\begin{aligned}\tau_n^H &= \Big[\frac{(\Delta t)}{2!}H_{tt} + \frac{(\Delta t)^2}{3!}H_{ttt} + \ldots\Big] - \theta\Big[\frac{2(\Delta x)^2}{4!}H_{xxxx} + \ldots \\ &\quad + \frac{2(\Delta y)^2}{4!}H_{yyyy} + \ldots\Big] \end{aligned} \tag{2.2.7}$$

$$\begin{aligned}\tau_n^V &= \Big[\frac{(\Delta t)}{2!}V_{tt} + \frac{(\Delta t)^2}{3!}V_{ttt} + \ldots\Big] - \theta\Big[\frac{2(\Delta x)^2}{4!}V_{xxxx} + \ldots \\ &\quad + \frac{2(\Delta y)^2}{4!}V_{yyyy} + \ldots\Big] \end{aligned} \tag{2.2.8}$$

$$\begin{aligned}\tau_n^C &= \Big[\frac{(\Delta t)}{2!}C_{tt} + \frac{(\Delta t)^2}{3!}C_{ttt} + \ldots\Big] - (H+V)D\Big[\frac{2(\Delta x)^2}{4!}C_{xxxx} + \ldots \\ &\quad + \frac{2(\Delta y)^2}{4!}C_{xxxx} + \ldots\Big] \end{aligned} \tag{2.2.9}$$

because,

$$H_t - \theta(H_{xx} + H_{yy}) - \phi + \tau H - m_x H = 0 \tag{2.2.10}$$

$$V_t - \theta(V_{xx} + V_{yy}) - \phi + \tau V - m_y V = 0 \tag{2.2.11}$$

$$C_t - (H+V)D[C_{xx} + C_{yy}] - \alpha(H+V) + \nu C = 0 \tag{2.2.12}$$

so, the truncation error for $\tau_n^H, \tau_n^V, \tau_n^C$ is of order $\mathcal{O}(\Delta t, (\Delta x)^2, (\Delta y)^2)$.

Chapter 3

Numerical Results

When modeling a physical event uncertainties can arise from countless sources (e.g. natural variation, measurement error, insufficient measurement techniques, etc.) In particular the accuracy of results is often complicated by the presence of uncertainties in experimental data that are used to estimate parameter values. It has been suggested that a way to improve the model for honeycomb construction is to test thoroughly the range of parameters and their relative importance [2]. We begin this chapter by stating the stationary solutions to the PDE system and observing the effect that the parameter values may have on these steady states. We list the four sets of initial conditions we consider for the system and conduct uncertainty and sensitivity analysis on a subset of the parameters for each initial condition at two different times. The uncertainty analysis (UA) investigates how much of the uncertainty in the model output can be attributed to uncertainties in the parameter inputs. The sensitivity analysis allows us to study how the variations in the model outputs can be attributed, either qualitatively or quantitatively, to different input sources [13].

3.1 Initial Conditions

Four different sets of initial conditions are considered:

$$\begin{aligned} H(x,y,0) &= F[e^{-Gx^2}+1] \text{ with } F=0.01 \text{ and } G=4, \\ V(x,y,0) &= 0.01 \text{ or some small value (because no y modulation)} \qquad (3.1.1) \\ C(x,y,0) &= 0.01 \text{ or some small value (because the initial wax distribution was thin} \end{aligned}$$

and flat.)

$$\begin{aligned} H(x,y,0) &= F[e^{-Gx^2}+1][e^{-Py^2}] \\ V(x,y,0) &= 0.01[e^{-Py^2}] \\ C(x,y,0) &= 0.01 \\ \text{with} & \quad F=0.01\ ;\ G=4\ ;\ P=0.01 \end{aligned} \qquad (3.1.2)$$

$$\begin{aligned} H(x,y,0) &= e^{-P(x^2+y^2)} \\ V(x,y,0) &= e^{-P(x^2+y^2)} \\ C(x,y,0) &= e^{-Py^2} \\ \text{with} & \quad P=0.1 \end{aligned} \qquad (3.1.3)$$

$$\begin{aligned} H(x,y,0) &= e^{-P(x^2+y^2)} \\ V(x,y,0) &= e^{-P(x^2+y^2)} \\ C(x,y,0) &= [1+sin(3x+\frac{\kappa}{2})]e^{-Py^2} \\ \text{with} & \quad P=0.01 \end{aligned} \qquad (3.1.4)$$

Notice for all sets of initial conditions we incorporate at least one exponential function. This is to mimic the elliptical shape of the honeycombs.

3.2 Parameter Estimation

3.2.1 Uncertainty Analysis- UA

The most common sampling based methods to perform UA are Monte Carlo methods. We will use a Latin hypercube sampling (LHS) technique because of its efficient implementation to draw our samples. LHS is a stratified sampling without replacement technique. A matrix is generated that consists of N rows, the number of stratifications, by K columns corresponding to the number of varied parameters [13]. N model solutions are then simulated, using each combination of parameter values. In general the LHS technique requires a smaller sample size than other Monte Carlo methods to achieve the same level of accuracy.

Example 1. Let $a \sim Unif(60, 90)$, $b \sim Unif(10, 50)$, and $c \sim Unif(0, 15)$. When n=5 one possible sampling from each bin is given by {60,68,72,81,85} for a, {15,24,31,41,43} for b, and {1,5,8,10,13} for c. A corresponding LHS is given by

$$C = \begin{bmatrix} 81 & 24 & 10 \\ 72 & 43 & 5 \\ 68 & 31 & 8 \\ 85 & 41 & 1 \\ 60 & 15 & 13 \end{bmatrix} \tag{3.2.1}$$

The purpose of UA in this thesis is to quantify the degree of confidence for our parameter values. We assume a uniform distribution for the parameters D, α, ν, θ, and τ. We then use a LHS technique to draw our samples for statistical analysis. We plot the outputs of mean wax, maximum wax, mean of XZ oriented bees, and mean of YZ oriented bees versus the sampled parameter values to check for monotonicity. The partial rank correlation coefficient (PRCC) measures the residuals from one parameter at a time while controlling for the effects of the other parameters. We use the PRCC, which is extremely effective at determining the sensitivity of highly monotonic parameters, to determine the strength of the relationship between the parameter values and the outputs. We set the significance level, α, at 0.05. If our p-value is less than α we reject the null hypothesis that the parameter value has no effect on the model and conclude that the PRCC value is statistically significant. The uniform distribution whence we draw our samples is given in Figure 3.2.1 and a sample LHS plot for the parameters of D, α, and ν is given in Figure 3.2.2.

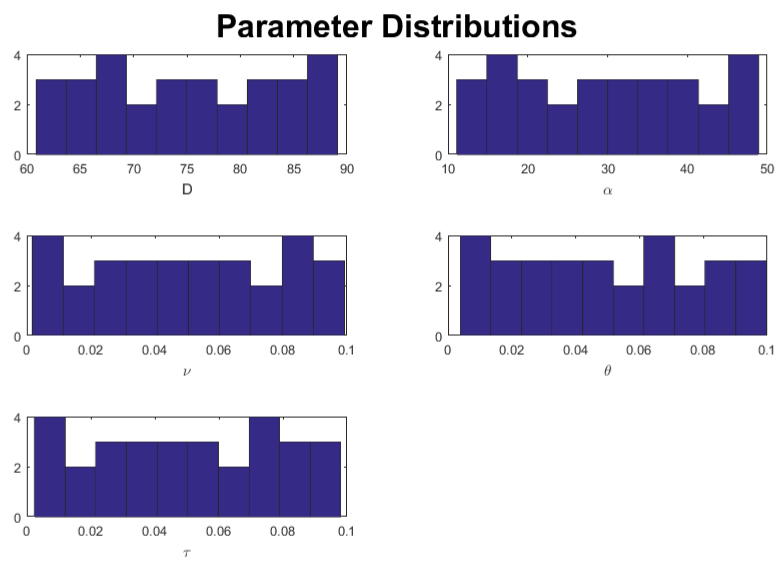

Figure 3.2.1: Uniform Distribution for Parameters D, α, ν, θ, and τ.

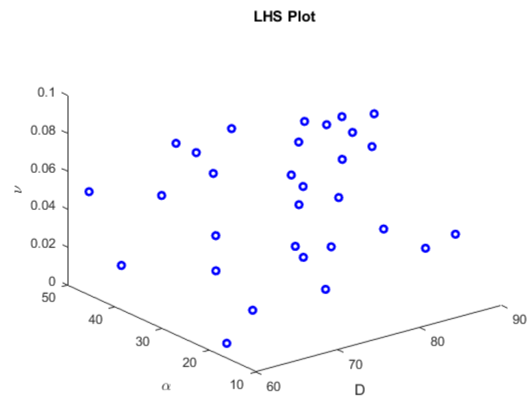

Figure 3.2.2: Sample LHS Plot for Paramters D, α, and ν.

In Figure 3.2.3, we see that for the output of mean wax concentration there is a positive correlation between the output and the parameters of D and ν; for the remaining parameters the correlation is negative. The plots of outputs versus parameters all display highly monotonic behavior with a single exception. This implies that overall the parameters from equations (1.1.1 - 1.1.3) are good candidates for a PRCC examination. The exception occurs in the plot of mean concentration of bees parallel to the XZ plane versus α. This plot begins by increasing until approximately $\alpha = 20$ then decreases for the remaining α values. For this particular case, it may have yielded more accurate results for the PRCC calculations if we ran the calculation separately for each interval.

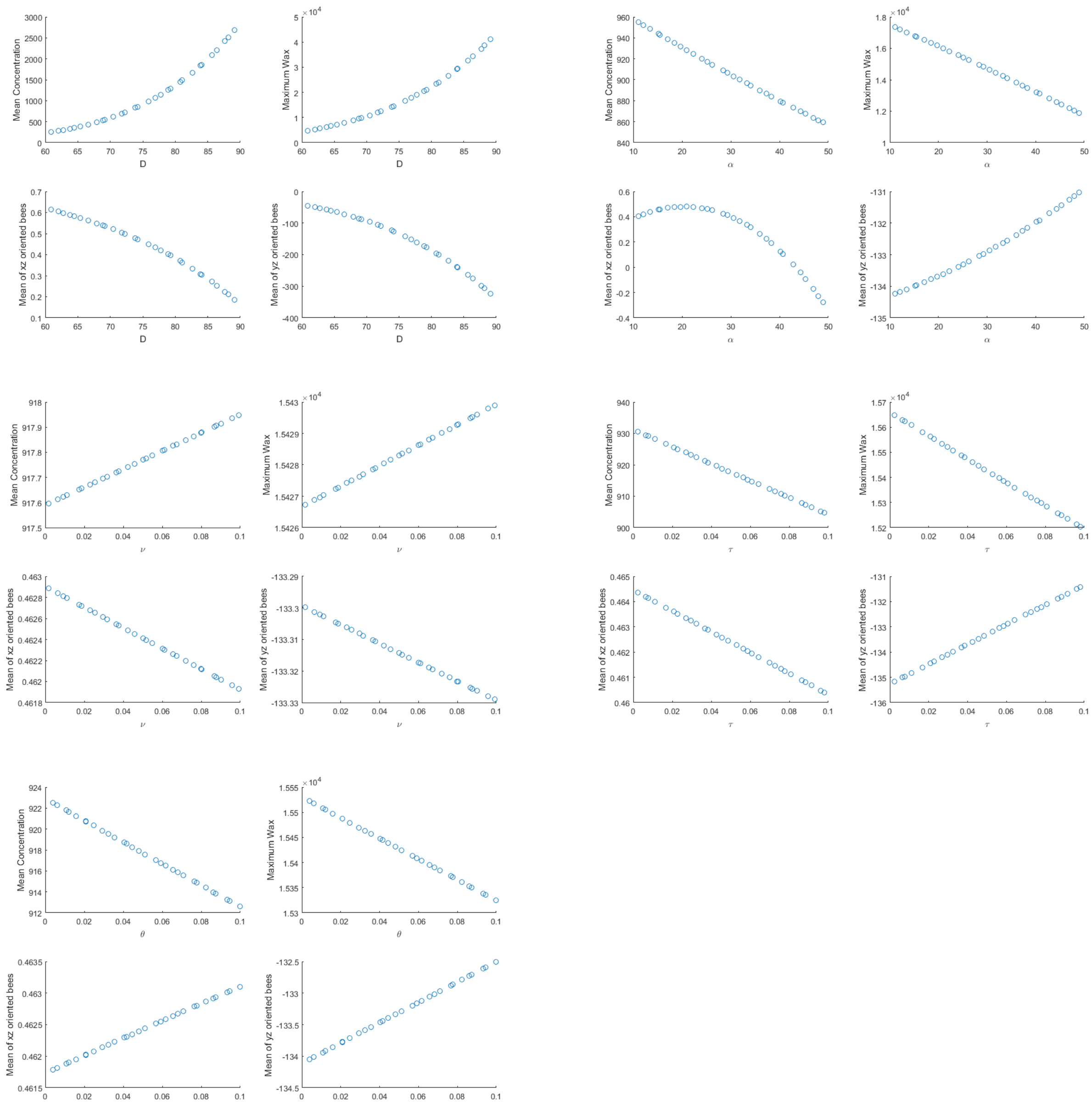

Figure 3.2.3: Monotonicity Plots for IC3 at t=0.2

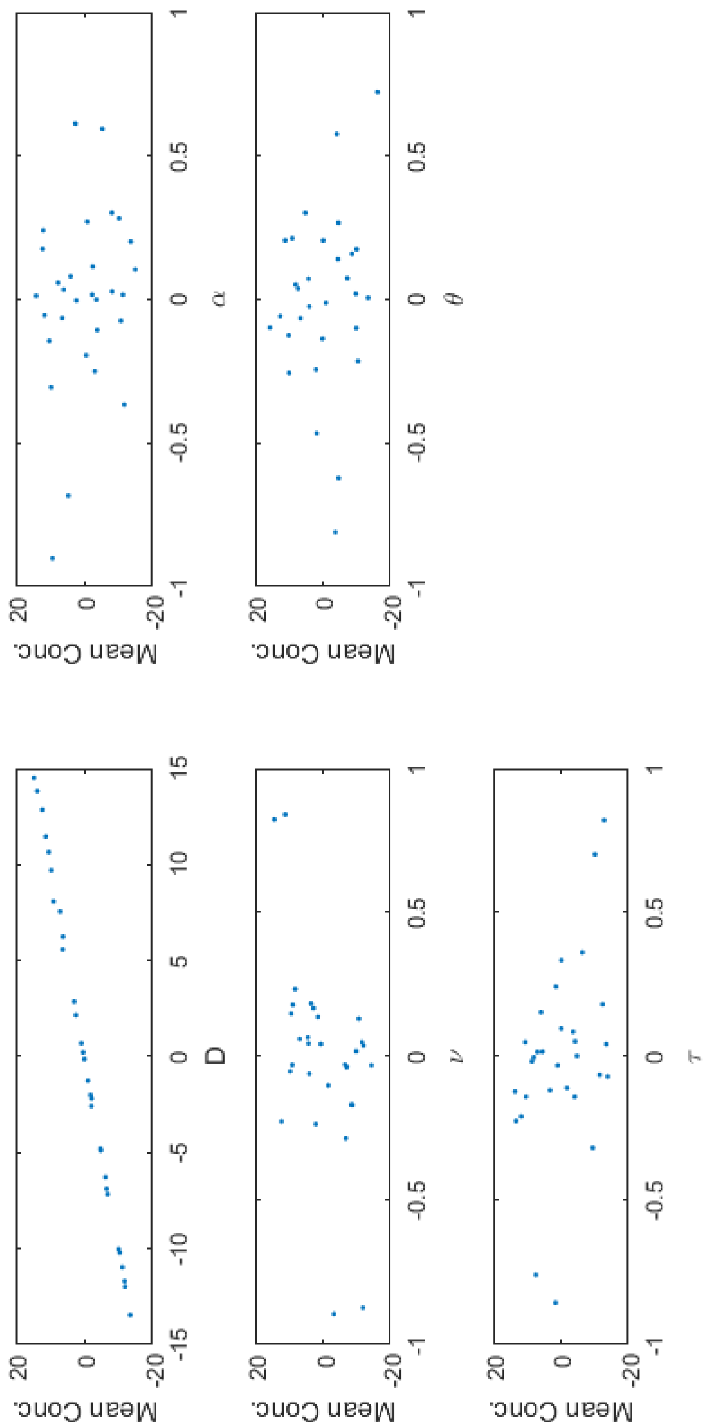

Figure 3.2.4: PRCC Plot of Mean Concentration for IC3 at t=0.2

Results: Experiment 1 - Initial Condition (3.1.1) at t=0.2

	Max. Wax		Mean Conc.		Mean XZ	
	PRCC	p-value	PRCC	p-value	PRCC	p-value
D	0.82288	2.39E-08*	0.58777	0.000637*	-0.93416	4.69E-14*
α	0.9831	3.43E-22*	0.99823	7.08E-36*	-0.98624	1.97E-23*
ν	-0.037513	0.84398	-0.13568	0.47467	-0.1379	0.4674
θ	-0.14521	0.4439	-0.21429	0.2555	0.085667	0.65263
τ	0.25684	0.17066	0.004734	0.98019	-0.2087	0.2684

	Mean YZ	
	PRCC	p-value
D	-0.096382	0.6124
α	0.96767	2.74E-18*
ν	0.11014	0.56233
θ	-0.06807	0.7208
τ	-0.98778	3.74E-24*

Table 3.1: Experiment 1 - Initial Condition (3.1.1) at t=0.2

We consider p-values less than 0.05 as statistically significant. We consider PRCC values greater than 0.75 as having a strong effect, between 0.5 and 0.75 as having a moderate effect, and between 0.25 and 0.5 as having a weak effect. The results given in Table 3.1 indicate that when the initial conditions for $V(x, y, 0)$ and $C(x, y, 0)$ are constant and the initial condition for $H(x, y, 0)$ only depends on x, as in (3.1.1), we find that the parameters that are statistically significant are D, α, and τ. In this experiment α has a strong effect on all the outputs, D has a strong effect on maximum wax concentration and mean density of bees parallel to the YZ plane, and τ has a strong effect on the mean density of bees parallel to the YZ plane. The effect of D on mean concentration of wax is moderate. The p-values larger than 0.05 indicate that with this set of initial conditions the parameters ν and θ do not affect the model. In this case, we conclude that overall α seems to be the parameter that most affects the outputs of the model.

Results: Experiment 2 - Initial Condition (3.1.2) at t=0.2

	Max. Wax		Mean Conc.		Mean XZ		Mean YZ	
	PRCC	p-value	PRCC	p-value	PRCC	p-value	PRCC	p-value
D	0.94885	1.59E-15*	0.93431	4.55E-14*	-0.92121	5.35E-13*	-0.7256	5.70E-06*
α	0.97424	1.19E-19*	0.98134	1.36E-21*	-0.98555	3.87E-23*	0.91622	1.22E-12*
ν	-0.0024312	0.98983	0.11171	0.55675	-0.099744	0.59999	0.28717	0.12389
θ	-0.049934	0.79329	-0.12337	0.51601	0.091145	0.63193	-0.0058422	0.97556
τ	-0.12077	0.52497	0.15385	0.41695	-0.22757	0.22649	-0.45545	0.011435*

Table 3.2: Experiment 2 - Initial Condition (3.1.2) at t=0.2

The results given in Table 3.2 indicate that when the initial condition for $V(x, y, 0)$ depends only on y, $C(x, y, 0)$ is constant, and $H(x, y, 0)$ depends on both x and y we can conclude that the effect of α is strong for all outputs. The effect of D is also strong for all outputs with one exception. For the output of the mean concentration of bees parallel to the YZ plane we find D has a moderate effect. We also find that τ has a weak effect for the output of the mean concentration of bees parallel to the YZ plane. P-values larger than 0.05 indicate that the parameters of ν and θ have no significant effects on the model. The parameter of α seems to have the strongest effect on the model overall when considering initial condition (3.1.2).

Results: Experiment 3 - Initial Condition (3.1.3) at t=0.2

Results for experiment 3 are given in Table 3.3. We find that the output of maximum wax concentration is strongly affected by the parameter D, moderately affected by α and weakly affected by θ. Mean wax concentration is also strongly affected by D and

	Max. Wax		Mean Conc.		Mean XZ	
	PRCC	p-value	PRCC	p-value	PRCC	p-value
D	0.99582	1.19E-30*	0.99937	4.19E-42*	-0.8784	1.77E-10*
α	-0.74466	2.37E-06*	-0.21254	0.25949	-0.90594	5.80E-12*
ν	0.31174	0.093539	0.47228	0.00841*	0.14993	0.42907
θ	-0.44699	0.013271*	-0.1567	0.40828	0.003316	0.98613
τ	0.029127	0.87857	-0.38721	0.034515*	0.008027	0.96642

	Mean YZ	
	PRCC	p-value
D	-0.99958	1.20E-44*
α	0.10712	0.57314
ν	-0.22794	0.22573
θ	0.20102	0.28681
τ	0.22759	0.22644

Table 3.3: Experiment 3 - Initial Condition (3.1.3) at t=0.2

weakly affected by ν and τ. The parameter α and then D both have a strong effect on the output of the mean concentration of bees parallel to the XZ plane. D is the only parameter that shows a statistically significant effect on the mean concentration of bees parallel to the YZ plane and the effect is strong. Overall it is worth emphasizing that for three out of four outputs the parameter of D has the strongest effect; and in all four cases the effect of D is considered strong. We conclude that for initial condition (3.1.3), D is the parameter that most affects the outputs of the model.

Results: Experiment 4 - Initial Condition (3.1.4) at t=0.2

The same initial conditions are used in experiment 4 as in experiment 3 with the alteration of multiplying the C(x,y,0) initial condition by a sinusoid. The results are given in Table 3.4. We now find that only the parameters of D and α are statistically significant. D has a perfect PRCC value of 1 for all outputs. The parameter α has a strong effect on all outputs. It is worth noting that for the output, mean concentration of bees parallel to the XZ plane, D and α seem to work opposite of one another. Both

	Max. Wax		Mean Conc.		Mean XZ	
	PRCC	p-value	PRCC	p-value	PRCC	p-value
D	1	0*	1	0*	1	0*
α	0.97424	1.19E-19*	0.98134	1.36E-21*	-0.98555	3.87E-23*
ν	-0.015278	0.93613	-0.015278	0.93613	-0.015278	0.93613
θ	0.1033	0.58698	0.1033	0.58698	0.1033	0.58698
τ	-0.12309	0.51696	-0.12309	0.51696	-0.12309	0.51696

	Mean YZ	
	PRCC	p-value
D	1	0*
α	0.91622	1.22E-12*
ν	-0.10678	0.57437
θ	0.11528	0.54412
τ	0.025614	0.89312

Table 3.4: Experiment 4 - Initial Condition (3.1.4) at t=0.2

have similar PRCC values in magnitude but with opposite direction (i.e. PRCC value of 1 for D versus PRCC value of -0.9855 for α.) We find the opposite effect for the mean concentration of bees parallel to the YZ plane. We conclude that for initial condition (3.1.4) both the parameters of D and α seem to have large effects on the model with the effect of D only slightly stronger.

Overall: Results at t=0.2

For two out of four experiments the parameter D is found to have the strongest effect overall on the system. In the two experiments where D is not the strongest parameter, α is found to have the greatest effect on the system. The parameters ν and θ are only significant when we consider initial condition (3.1.3) and both of their effects we categorize as weak. It is worth noting how the effect of parameter τ changes based on the initial condition considered. With initial condition (3.1.3) it has a weak effect on the mean concentration of wax, with initial condition (3.1.2) it has a weak effect on the mean density of bees parallel to the YZ plane, with initial condition (3.1.1) it has a strong effect on the mean density of bees parallel to the YZ plane, and with initial condition (3.1.4) it has no significant effect.

Results: Experiment 1 - Initial Condition (3.1.1) at t=0.4

	Max. Wax		Mean Conc.		Mean XZ	
	PRCC	p-value	PRCC	p-value	PRCC	p-value
D	0.92228	4.44E-13*	0.91854	8.38E-13*	-0.89821	1.67E-11*
α	0.98604	2.41E-23*	0.98532	4.81E-23*	-0.98545	4.28E-23*
ν	0.098365	0.60506	0.080178	0.67363	-0.11669	0.53916
θ	-0.22033	0.24202	-0.23317	0.21495	0.30431	0.10205
τ	0.21902	0.24491	0.17158	0.36463	-0.20938	0.2668

	Mean YZ	
	PRCC	p-value
D	0.3317	0.073342
α	0.98563	3.59E-23*
ν	0.053371	0.7794
θ	-0.30102	0.106
τ	-0.97639	3.55E-20*

Table 3.5: Experiment 1 - Initial Condition (3.1.1) at t=0.4

The results for initial conditions (3.1.1) at t = 0.4 can be found in Table 3.5. We find similar results to those at t = 0.2. The parameter α seems to make the greatest contribution. It has a strong effect on all outputs and D, as well, has a strong effect for all outputs with the exception of the mean density of bees parallel to the YZ plane.

Results: Experiment 2 - Initial Condition (3.1.2) at t=0.4

	Max. Wax		Mean Conc.		Mean XZ	
	PRCC	p-value	PRCC	p-value	PRCC	p-value
D	0.92121	5.35E-13*	0.93593	3.24E-14*	-0.91854	8.387E-13*
α	0.98555	3.87E-23*	0.98447	1.06E-22*	-0.98532	4.81E-23*
ν	0.099744	0.59999	0.17093	0.36647	-0.080178	0.67363
θ	-0.091145	0.63193	-0.15775	0.40509	0.23317	0.21495
τ	0.22757	0.22649	0.17158	0.13072	-0.17158	0.36463

	Mean YZ	
	PRCC	p-value
D	-0.93045	9.89E-14*
α	-0.9866	1.369E-23*
ν	-0.10841	0.56852
θ	0.06645	0.72718
τ	-0.21131	0.26233

Table 3.6: Experiment 2 - Initial Condition (3.1.2) at t=0.4

The results for initial condition (3.1.2) at time t = 0.4 can be found in Table 3.6. The only parameters that are found to have an effect on the outputs of the model are D and α and they have a strong effect on all of the outputs. It is worth noting that as the time increased from t = 0.2 to 0.4 the effect of D on the mean concentration of bees parallel to the YZ axis increased from moderate to strong and the effect of τ, which was weak previously, is now not significant.

Results: Experiment 3 - Initial Condition (3.1.3) at t=0.4

The results for experiment 3 are given in Table 3.7. We find that when we double the time, all parameters are now found to be statistically significant in contributing to the outputs of maximum wax concentration and the mean density of bees parallel to the YZ plane. For both of the outputs D and α have a strong effect, whereas τ, ν, and θ have a weak effect. When we examine the mean concentration of wax, we find

	Max. Wax		Mean Conc.		Mean XZ	
	PRCC	p-value	PRCC	p-value	PRCC	p-value
D	0.99577	1.42E-30*	0.9963	2.1457E-31*	-0.86172	9.63E-10*
α	0.88422	9.2579E-11*	0.74113	2.8064E-06*	-0.95342	4.1645E-16*
ν	0.38213	0.03717*	0.20599	0.27481	0.057747	0.76181
θ	-0.37707	0.039971*	-0.29967	0.10766	-0.020161	0.91578
τ	-0.40108	0.028046*	-0.34706	0.060243	-0.067066	0.72475

	Mean YZ	
	PRCC	p-value
D	-0.99583	1.1418E-30*
α	-0.88974	4.8438E-11*
ν	-0.37638	0.040367*
θ	0.38998	0.033136*
τ	0.46148	0.01026*

Table 3.7: Experiment 3 - Initial Condition (3.1.3) at t=0.4

D has a strong effect and α has a moderate effect. For the output of mean density of bees parallel to the XZ plane both D and α have a strong effect.

Results: Experiment 4 - Initial Condition (3.1.4) at t=0.4

The results for (3.1.4) can be found in Table 3.8. In comparison to time t = 0.2, D is still found to have a strong effect with a perfect PRCC value, but now the effect of α is not found to be significant.

Overall: Results at t=0.4

For all initial conditions the parameter D has a strong effect on the model with the single exception of, initial condition (3.1.1), mean density of bees parallel to the YZ plane in which case the D is not found to be significant. Excluding initial condition (3.1.4), the parameter α has a strong effect on the model for all initial conditions considered with the one exception of, initial condition (3.1.3), mean concentration

	Max. Wax		Mean Conc.		Mean XZ	
	PRCC	p-value	PRCC	p-value	PRCC	p-value
D	1	0*	1	0*	1	0*
α	-0.015278	0.93613	-0.015278	0.93613	-0.015278	0.93613
ν	-0.27584	0.1401	-0.27584	0.1401	-0.27584	0.1401
θ	0.1033	0.58698	0.1033	0.58698	0.1033	0.58698
τ	-0.12309	0.51696	-0.12309	0.51696	-0.12309	0.51696

	Mean YZ	
	PRCC	p-value
D	-1	0*
α	-0.10678	0.57437
ν	-0.042302	0.82435
θ	0.11528	0.54412
τ	0.025614	0.89312

Table 3.8: Experiment 4 - Initial Condition (3.1.4) at t=0.4

of wax, in which case the effect of α is moderate. For initial condition (3.1.3), the remaining parameters, ν, θ, and τ, each have a weak effect on the outputs of maximum concentration of wax and mean density of bees parallel to the YZ plane.

3.2.2 Sensitivity Analysis- SA

SA can be used in the field of numerical simulation, where mathematical and computational models are used for the study of systems, especially complex ones. SA helps to understand the behavior of a model, the coherence between a model and the world, and how different parts of the model interplay [5]. SA provides a way to identify which model inputs have the strongest effect on the uncertainty in the model predictions. SA can be divided into two compartments, local and global. Local SA methods are used when input parameters are relatively certain. When larger finite regions for the parameters values need to be explored global SA methods are implemented. Several different approaches have been attempted for global sensitivity analysis, due to the intrinsic difficulty of building an effective and rigorous measurement over a finite space of variation for the inputs. In this thesis we use the global SA method of an extended Fourier amplitude test.

eFAST developed by Saltelli and Bolado is based on the original FAST. eFAST is a variance decomposition method where input parameters are varied causing variation in model output. The variation is quantified using the statistical notion of variance $s^2 = \sum_{i=1}^{N}(y_i - \bar{y})^2/(N-1)$, where N = sample size, y_i = ith model output, and $\bar{y}$ = sample mean. The algorithm then partitions the output variance, determining what fraction of the variance can be explained by variation in each input parameter. Partitioning of variance in eFAST works by varying different parameters at different frequencies, encoding the identity of parameters in the frequency of their variation. Fourier analysis then measures the strength of each parameter's frequency in the model output. Thus, how strongly a parameter's frequency propagates from input, through the model, to the output serves as a measure of the model's sensitivity to the parameter. Using eFAST we are able to calculate both the first order sensitivity and the total order sensitivity for any chosen parameter. A first order sensitivity index, S_i, of a given parameter i, is calculated as the variance at a particular parameter's unique frequency divided by total variance. First variance s_i^2 is calculated from the Fourier coefficients at the frequency of interest, j: $s_i^2 = 2(A_j^2 + B_j^2)$ where $A_j = \frac{1}{\pi}\int_{-\pi}^{\pi} f(x)cos(jx)dx$ and $B_j = \frac{1}{\pi}\int_{-\pi}^{\pi} f(x)sin(jx)dx$. The first order $S_i = s_i^2/s_{total}^2$. This index represents the fraction of model output variance explained by the input variation of a given parameter. To estimate the total order sensitivity index, S_{Ti}, of a given parameter i, eFAST first calculates the summed sensitivity index of the entire complementary set of parameters. S_{Ti} is then calculated as the remaining variance after the contribution of the complementary set,S_{ci}, is removed, so $S_{Ti} = 1 - S_{ci}$. Using this method we are able to rank the parameters and determine which have the strongest effect on the model. A dummy variable is put to use with the eFAST method to test for statistical significance. Parameters with a total order sensitivity index less than or equal to that of the dummy variable should be considered not significantly different from zero. The eFAST method also computes the coefficient of variation (CV) for both the S_i and S_{Ti}. CV measures the dispersion of the data relative to the mean.

Experiment 1

The eFAST results for the simulation carried out for mean wax concentration at t = 0.2 are provided in the tables below.

Parameter i	D	α	ν	θ	τ	d
S_i	0.0024	0.9942	0.0000	0.0000	0.0000	0.0000
S_{T_i}	0.0067	0.9976	0.0024	0.0025	0.0026	0.0024
CV(S_i)	5.0486	0.1580	27.2939	96.9980	19.0110	107.9855
CV(S_{T_i})	22.2578	0.0726	6.7396	10.0116	13.0809	9.1359

Table 3.9: Effect on mean wax concentration at $t = 0.2$ initial condition (3.1.1)

Parameter i	D	α	ν	θ	τ	d
S_i	0.2341	0.6352	0.0001	0.0004	0.0002	0.0002
S_{T_i}	0.3480	0.7648	0.0021	0.0057	0.0025	0.0034
CV(S_i)	1.1587	3.8220	49.6036	116.4429	66.2438	93.1258
CV(S_{T_i})	1.8913	1.1634	90.2786	70.3906	83.6615	46.9087

Table 3.10: Effect on mean wax concentration at $t = 0.2$ initial condition (3.1.2)

Parameter i	D	α	ν	θ	τ	d
S_i	0.9941	0.0023	0.0002	0.0003	0.0005	.0003
S_{T_i}	0.9983	0.0077	0.0046	0.0053	0.0054	.0048
CV(S_i)	0.1034	44.2524	6.5588	38.7963	40.2168	10.7366
CV(S_{T_i})	0.0256	28.3289	7.5820	7.3305	9.9322	5.6942

Table 3.11: Effect on mean wax concentration at $t = 0.2$ initial condition (3.1.3)

Parameter i	D	α	ν	θ	τ	d
S_i	0.9926	0.0005	0.0005	0.0005	0.0005	0.0005
S_{T_i}	0.9995	0.0078	0.0077	0.0076	0.0073	0.0074
CV(S_i)	0.0229	6.6225	5.5411	4.2270	3.0846	7.1046
CV(S_{T_i})	0.0029	3.5772	2.9626	2.3241	1.3876	3.6360

Table 3.12: Effect on mean wax concentration at $t = 0.2$ initial condition (3.1.4)

Experiment 2

The eFAST results for the simulation carried out for mean wax concentration at t = 0.4 are provided in the tables below.

Parameter i	D	α	ν	θ	τ	d
S_i	0.1723	0.6805	0.0004	0.0008	0.0005	0.0005
S_{T_i}	0.3163	0.8277	0.0056	0.0067	0.0050	0.0053
CV(S_i)	4.5728	5.0559	66.0955	100.8445	86.3217	52.3576
CV(S_{T_i})	7.1874	1.6628	64.2175	29.1694	41.4134	52.1178

Table 3.13: Effect on mean wax concentration at $t = 0.4$ initial condition (3.1.1)

Parameter i	D	α	ν	θ	τ	d
S_i	0.1970	0.6771	0.0002	0.0013	0.0006	0.0004
S_{T_i}	0.3347	0.8065	0.0037	0.0107	0.0080	0.0061
CV(S_i)	3.5097	2.2886	21.0124	62.3198	43.5403	48.0610
CV(S_{T_i})	5.3644	0.2529	40.4682	52.9186	53.0907	51.8937

Table 3.14: Effect on mean wax concentration at $t = 0.4$ initial condition (3.1.2)

Parameter i	D	α	ν	θ	τ	d
S_i	0.9674	0.0164	0.0002	0.0004	0.0010	0.0002
S_{T_i}	0.9829	0.0282	0.0050	0.0049	0.0058	0.0047
CV(S_i)	0.3515	14.7665	32.9325	62.6571	45.2834	16.5077
CV(S_{T_i})	0.1882	26.6968	21.9682	9.0098	26.0924	18.3368

Table 3.15: Effect on mean wax concentration at $t = 0.4$ initial condition (3.1.3)

Parameter i	D	α	ν	θ	τ	d
S_i	0.9927	0.0005	0.0005	0.0005	0.0005	0.0005
S_{T_i}	0.9995	0.0073	0.0073	0.0074	0.0076	0.0077
CV(S_i)	0.0247	5.3317	4.4518	6.1752	10.0265	5.5878
CV(S_{T_i})	0.0030	2.5252	2.3227	3.1673	5.2370	3.0471

Table 3.16: Effect on mean wax concentration at $t = 0.4$ initial condition (3.1.4)

Results - Experiment 1

The results for experiment 1 are given in Tables 3.9 - 3.12. For all parameters the total effects are stronger than the individual effects. We use the S_i and S_{ti} values larger than the dummy variable to rank the parameters effects. For initial conditions (3.1.3) and (3.1.4), D by far has the strongest total effect followed by α. In the former, τ and θ are found to be significant; in the latter, ν and θ are found to be significant. For initial condition (3.1.4) D is the only parameter with an individual effect. For initial conditions (3.1.1) and (3.1.2), α followed by D have the most substantial effects.

Results - Experiment 2

The results for experiment 2 are given in Tables 3.13 - 3.16. When the time is increased to t = 0.4 , although we still have D with the leading effect for initial condition (3.1.3) for both S_i and S_{ti}, its effect starts to decrease and the other parameters increase their effects. We see the same pattern with initial condition (3.1.1). The previous leading parameter, in this case α, keeps its position as leading parameter, but its effect starts to decrease and the effects of the other parameters begin to increase. The opposite happens with initial condition (3.1.4). The effect of the leading parameter D increases or stays the same and both the individual and total effects for all other parameters become no longer significant. For initial condition (3.1.2) α keeps its position as the leading parameter and continues to increase its effect while all other parameters except for D also increase their effects. Although the total effect of D does decrease it keeps its position as the parameter with the second strongest effect. Overall, with the exception of initial condition (3.1.4), with an increase in time we see an increase in the effect of the parameters on the model.

Chapter 4

Actual Honey Combs versus Models

4.1 Ratios of Major to Minor Axis

Figure 4.1.1: Wild hive displaying a parallelism between combs

It is evident that honeycombs display an elliptical form during stages of construction. And it has been stated in the literature that the construction of honeycomb is not a random process, but follows the mathematical rules involving the golden ratio [9]. We begin this chapter by searching for circumstantial evidence that the elliptical

Figure 4.1.2: Individual elliptical combs

honeycomb is based on the golden ratio, ϕ, $\frac{1+\sqrt{5}}{2} \approx 1.6180339$. Comb measurement were gathered from a top bar hive in Milan, Tennessee. At the beginning of comb construction the top bar hive plays the role of a foundationless frame mimicking a wild comb. Digital images were taken of each comb. Software was then used to manually fit an ellipse to each comb from which we extracted the ratio of the length of the major axis to the length of the minor axis. Seven combs were found displaying an elliptical shape and five samples were drawn from each comb. The results are given in Table 4.1.

The data was found to have a mean of 1.412044 with a standard deviation of 0.278535.

Comb1		Comb 2		Comb 3		Comb 4	
SMP	Ratio	SMP	Ratio	SMP	Ratio	SMP	Ratio
1	1.386100386	1	1.207594937	1	1.134433962	1	1.057603687
2	1.456349206	2	1.207594937	2	1.157107232	2	1.24929972
3	1.451361868	3	1.208121827	3	1.116113744	3	1.13559322
4	1.36437247	4	1.050239234	4	1.110849057	4	1.178484108
5	1.453488372	5	1.194835681	5	1.229885057	5	1.156097561

Comb 5		Comb 6		Comb 7	
SMP	Ratio	SMP	Ratio	SMP	Ratio
1	1.355163728	1	1.856115108	1	1.815789474
2	1.37913486	2	1.962962963	2	1.694736842
3	1.359693878	3	1.904411765	3	1.988235294
4	1.394402036	4	1.714285714	4	1.6
5	1.364102564	5	1.776978417	5	1.75

Table 4.1: Ratios of major axis to minor axis for combs sampled

4.2 Elliptical Fits

Figure 4.2.1 gives a graph of the model from equations (1.1.1) - (1.1.5) with initial condition (3.1.3) at time t = 0.2. To emphasize the elliptical nature of the output we extract cross sections in both directions of the XY plane. The resulting graphs are given in Figures 4.2.1 and 4.2.2. The elliptical nature of the wax concentration is most evident with cross sections taken at $y \approx 0$ and $y \approx 1.25$. We used a least squares minimization to fit an ellipse to numerical data [10]. Notice in Figure 4.2.2 the difference between the exact point located on the graph of wax concentration and the point used for fitting the ellipse. For the cross section at $y \approx 0$ the discrepancies are minimal. We see a very good elliptical fit. For the cross section at $y \approx 1.25$, corresponding to the second honey comb, the fit is not as good.

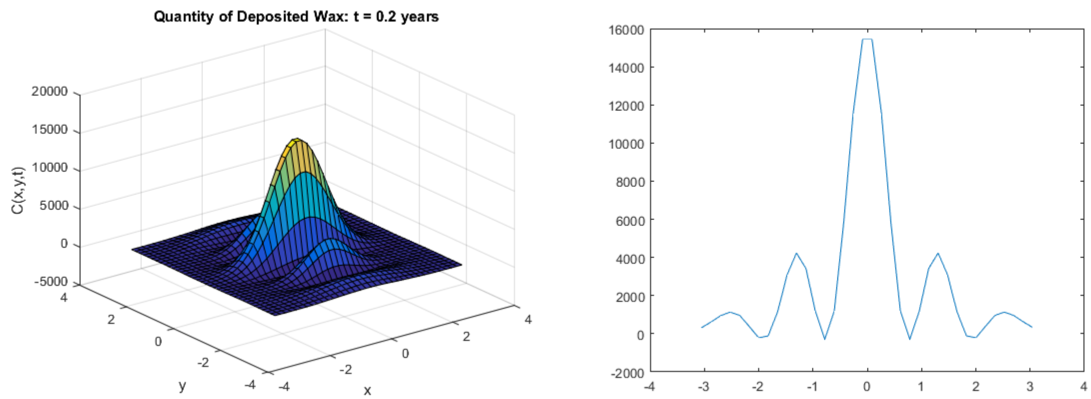

Figure 4.2.1: Wax concentration and cross section at $x \approx 0$

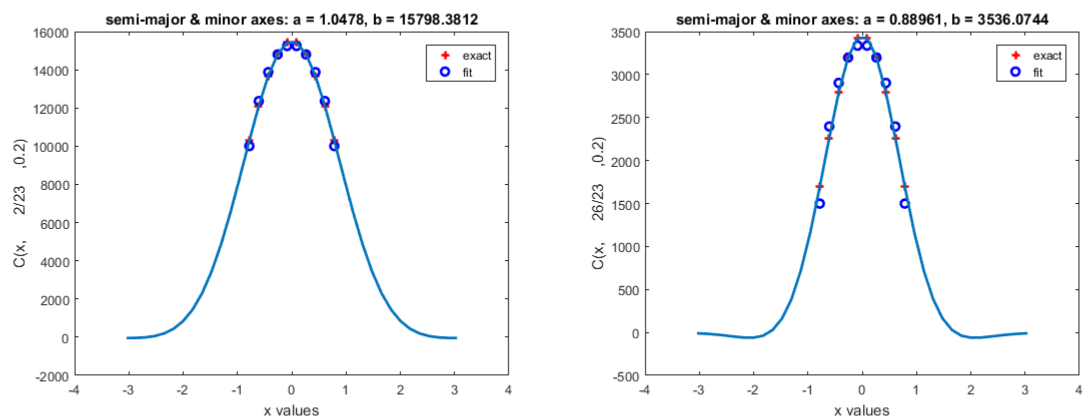

Figure 4.2.2: Cross sections at $y \approx 0$ and $y \approx 1.25$

4.3 Conclusions

In Chapter 3, we saw that for initial conditions (3.1.3) and (3.1.4) the parameter of D had the strongest overall effect on the model. In this section we examine the outputs of the model for varying D values at time t = 0.2 and t = 0.4. Figure 4.3.1 compares two different D values for initial condition (3.1.3). It is clear that the D value of 50 better captures the tendency of bees to mimic each other so that the vast majority will concentrate in one direction, in this case, parallel to the XZ plane. Also we get an output of wax concentration that resembles elliptical combs. From Figure 4.3.2 we see that when we increase the time to t = 0.4 the average density of bees that are working decreases and the parallelism in the concentration of wax becomes evident.

In Figure 4.3.3 we increase the D value to 75 and compare the outputs for initial condition (3.1.3) and (3.1.4) at time t = 0.4. We see that at this value of D the model for the former initial condition begins to break down because the side combs become taller than the middle comb. This is not consistent with what we know of hive construction. We conclude in this case that the latter initial condition best captures the nuances of honeycomb construction.

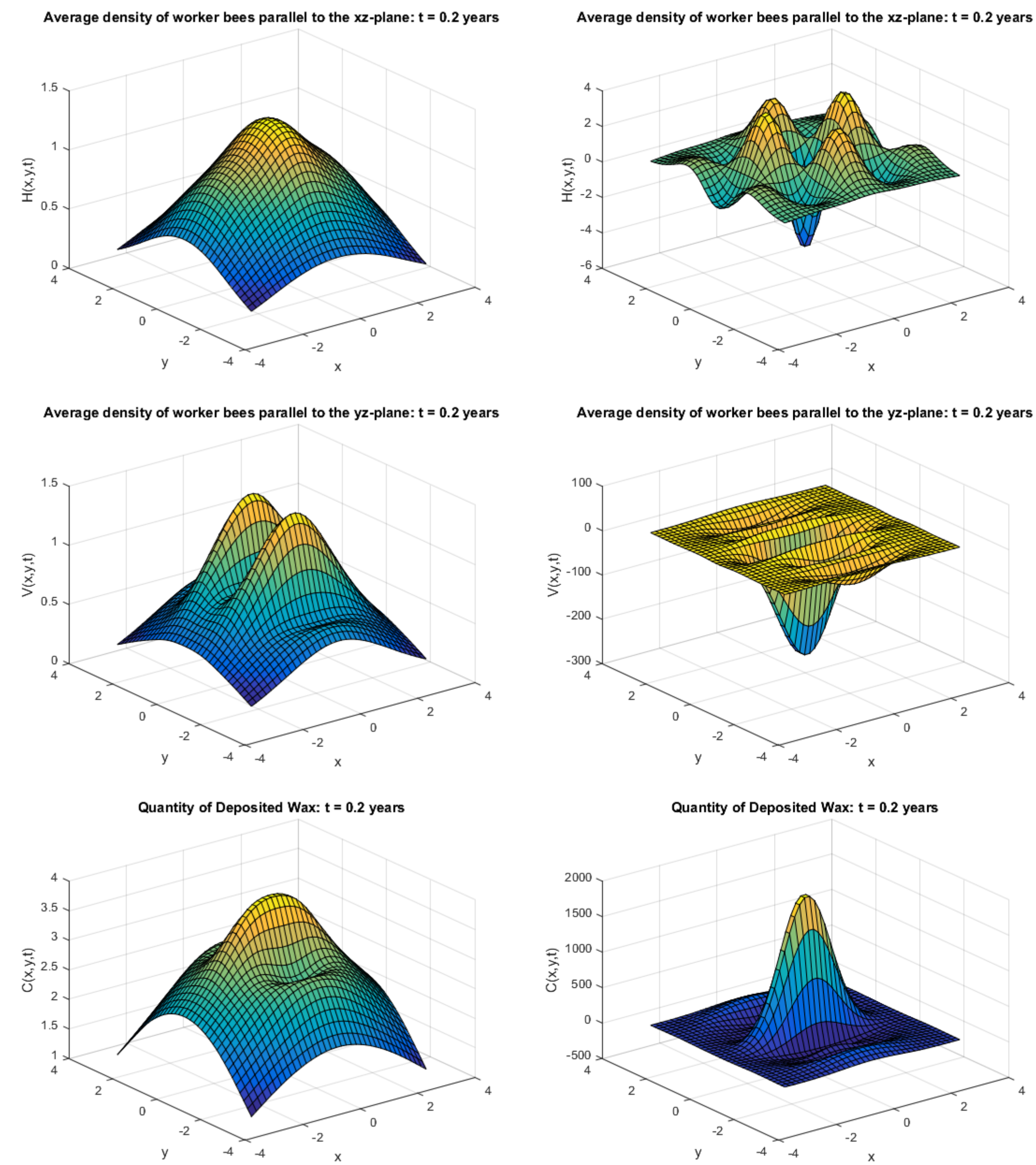

Figure 4.3.1: Model at t=0.2: D=10 and D=50; initial condition (3.1.3)

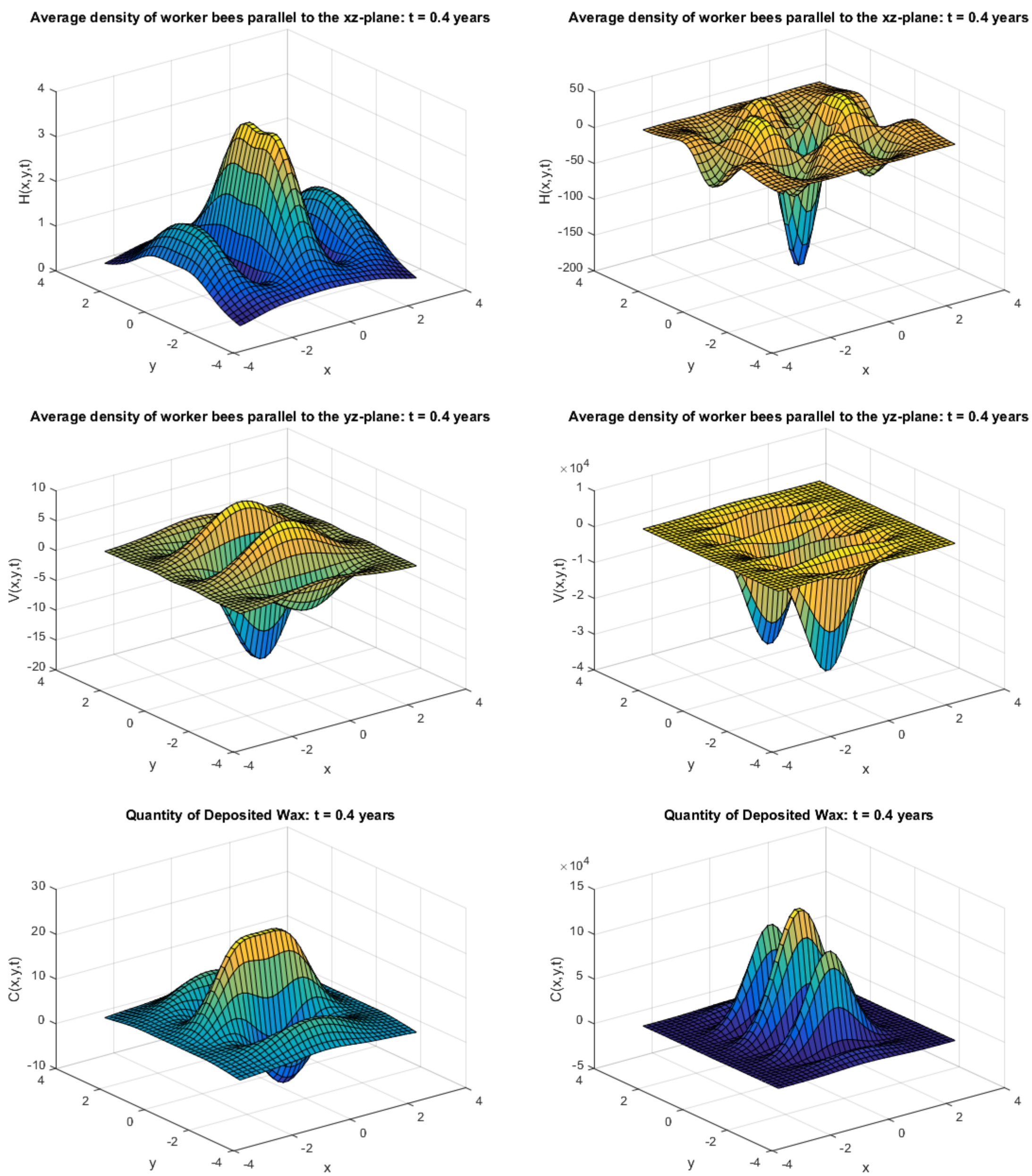

Figure 4.3.2: Model at t=0.4: D=10 and D=50; initial condition (3.1.3)

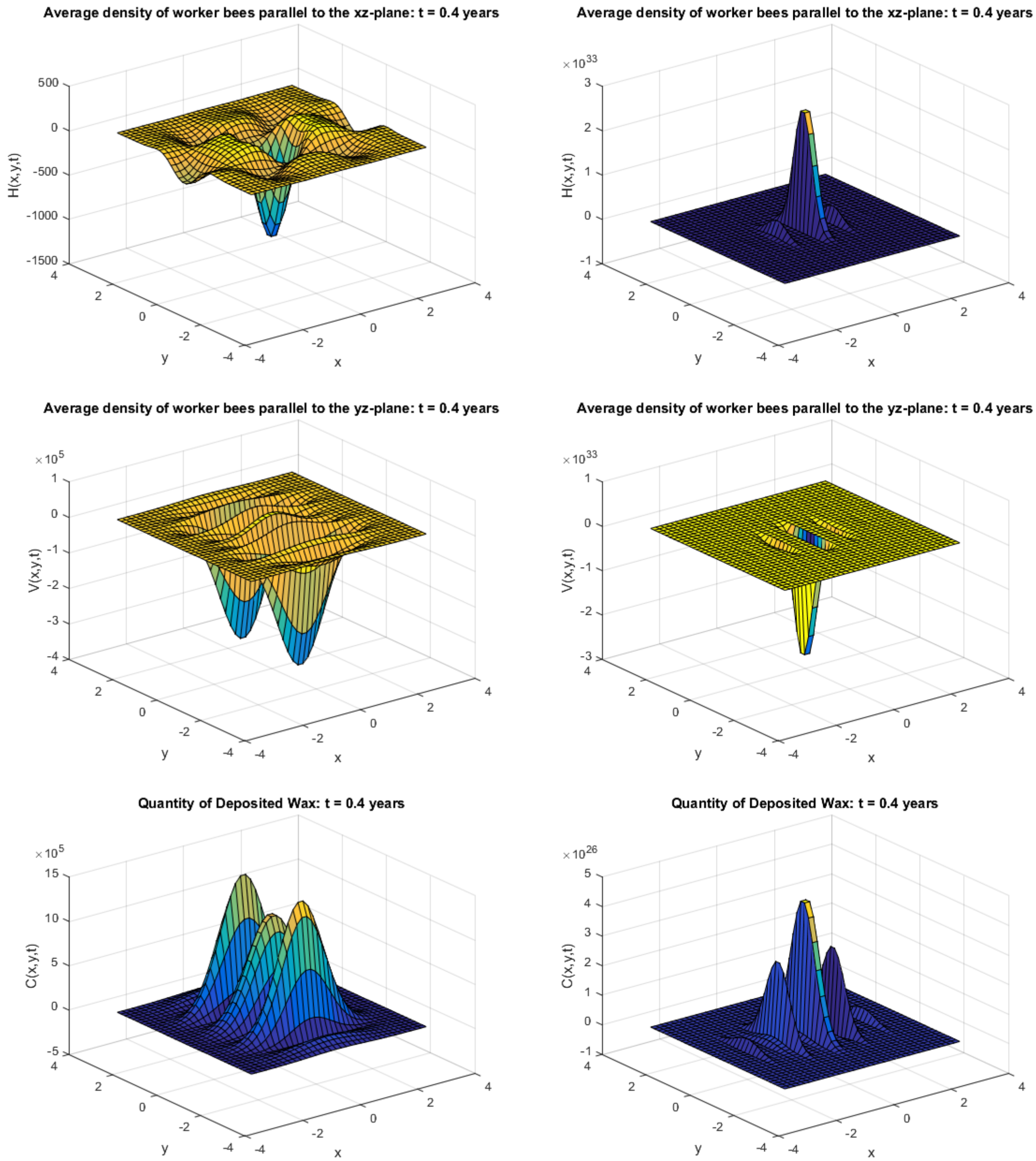

Figure 4.3.3: Model at t=0.4 with D=75; initial condition (3.1.3) and (3.1.4)

References

[1] Baldwin, Stuart A.: Some historical aspects of honeycomb mathematics. Bee Craft Digital (2012) 27-30

[2] Bélic, M., Deneubourg, J., Škarka, V.: Mathematical model of honeycomb construction. J. Math. Biol. (1986) 24: 437-449.

[3] Broed, Robert, Ekström: Sensitivity analysis methods and a biosphere test case implemented in EIKOS (2006)

[4] Camazine, Scott: Self-organizing pattern formation on the combs of honey bee colonies. Behav Ecol Sociobiol (1991) 28:61-76.

[5] Chan, K.P.-S., Tarantola, S., Saltelli, A.: A quantitative model-independent method for global sensitivity analysis of model output. Technometrics (2012) 41:1, 39-56

[6] Collins, Joseph C. III: Latin hypercube sampling in sensitivity analysis. Amry Research Laboratory (1994)

[7] Dolicanin, D. C., Nikolic, V. B., Dolicanin, C.B.: Application of finite difference method to study of the phenomenon in the theory of thin plates. Appl. Math. Inform, and Mech. vol. 2,1 (2010), 29-43.

[8] Egami, Takeshi, Bultheel, Adhemar, Kaatz, Forrest H.: Order of parameters from image analysis: a honeycomb example. Naturwissenschaften (2008) 95:1033-1040.

[9] Favre, Daniel: Golden ratio (*Sectio Aurea*) in the elliptical honeycomb. J. of Nature and Science 2(1):e173 (2016).

[10] Flusser, Jan, Halir, Radim Numerically stable direct least squares fitting of ellipses.

[11] Frey, H. Christopher, Mokhtari, Amirhossein: Volume 2: Evaluation and recommendation of methodology for conducting sensitivity analysis in probabilistic models. Review and Reccomendation of methods for sensitivity and uncertainty analysis for the stochastic human exposure and dose simulation models. (2005)

[12] Gallai, N., Salles, J.M., Settele, J., Vaissiere, B. Economic valuation of the vulnerability of world agriculture confronted with pollinator decline Ecological Economics 68 (2009)

[13] Kirschner, Denise, Ray, Christian J., Hogue, Ian B., Marino, Simeone: A methodology for performing global uncertainty and sensitivity analysis in systems biology. Journal of Theoretical Biology (2008) 178-196

[14] Kurstjens, S.P., Hepburn, H.R.: The combs of honeybees as composite materials. Apidologie, Springer Verlag, (1988) 19 (1):25-36

[15] Lax, M., Deneubourg, J., Škarka, V., Bélic, M.: Mathematical model of honeycomb construction. J. Math. Biol. (1986) 24: 437-449.

[16] Mingham, C.G., Causon, D.M.: *Introductory Finite Difference Methods for PDEs*. Ventus Publishing ApS (2010).

[17] Petzold, Linda, Li, Shengtai: Adjoint sensitivity analysis for time-dependent partial differential equations with adpative mesh refinement. Journal of Computational Physics 198 (2004) 310-325

[18] Radloff, S.E., Hepburn, H.R., Pirk, C.W.W.: Honeybee combs: construction through a liquid equilibrium process? Naturwissenschaften (2004) 91:350-353

[19] Serban, Radu, Cao, Yang, Li, Shengtai, Petzold, Linda: Sensitivity analysis of differential-algebraic equations and partial differential equations. (2006)

[20] Tepedino, V.J. The importance of bees and other insect pollinators in maintaining floral species composition Great Basin Naturalist Memoirs No.3 The endangered species: A symposium (1979)